



Dynamic Mode Decomposition Uncovers Hidden Oceanographic Features Around the Strait of Gibraltar

Sudam Surasinghe¹, Sathsara Dias¹, Kanaththa Priyankara¹, Erik Bollt^{1,2},
Marko Budišić¹, Larry Pratt³ and Jose Sanchez-Garrido⁴.

¹ Department of Mathematics, Clarkson University, Potsdam, NY 13699, USA

² Department of Electrical and Computer Engineering, Clarkson Center for Complex Systems Science (C³S²), Clarkson University, Potsdam, NY 13699, USA

³ Woods Hole Oceanographic Institution, Woods Hole, Massachusetts, USA

⁴ Physical Oceanography Group, University of Malaga, Campus de Teatinos s/n, 29071 Malaga, Spain

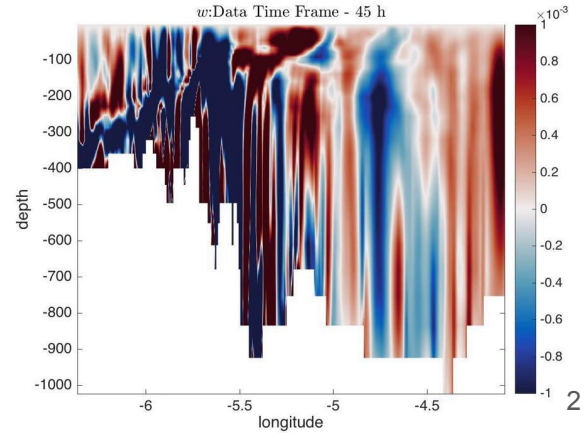
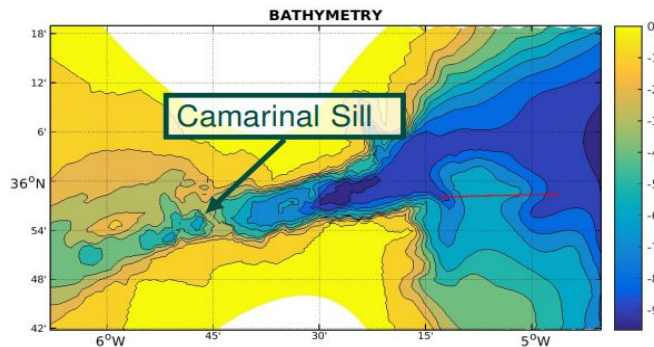
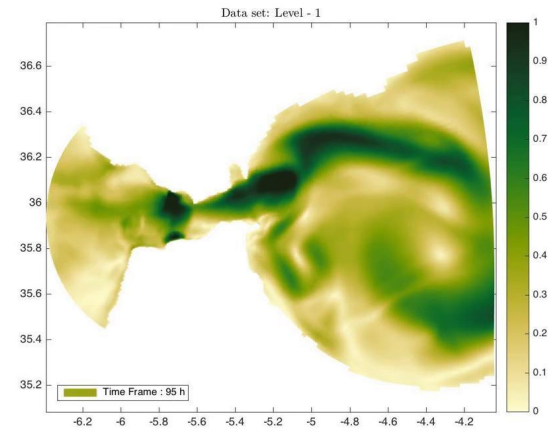
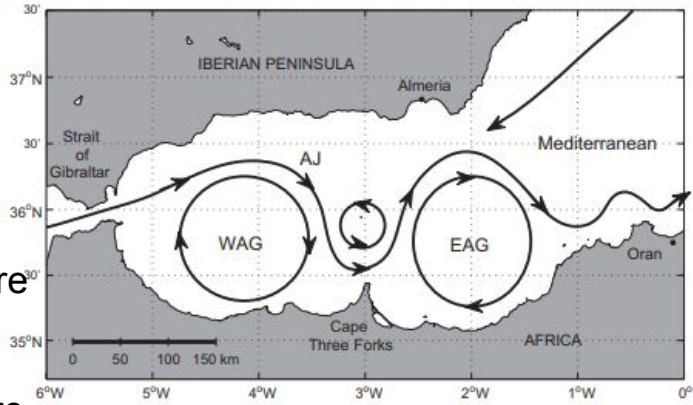
Presented in 73rd Annual Meeting of the APS Division of Fluid Dynamics,
Session H10: Geophysical Fluid Dynamics: Oceanographic,
Sunday, November 22–24, 2020; Virtual, CT (Chicago time) 5:45pm - 6:30pm.

Strait of Gibraltar and Western Mediterranean

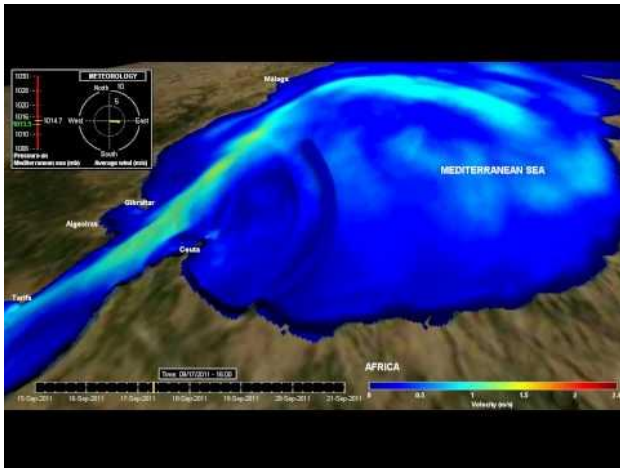
- AJ - Atlantic Jet
- WAG - Western Alboran Gyre
- EAG - Eastern Alboran Gyre
- Camarinal Sill (CS): Underwater elevation where an internal hydraulic jump gives rise to

- internal waves comprising solitons
- internal tides.

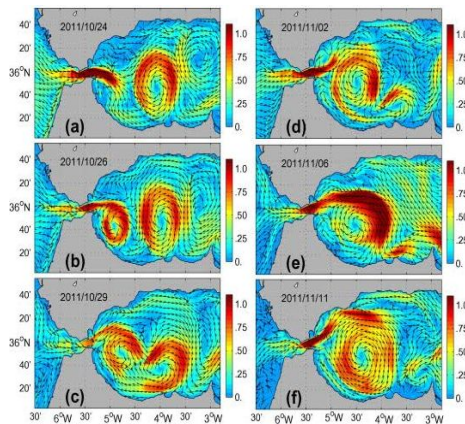
[Sánchez-Garrido, 2013]



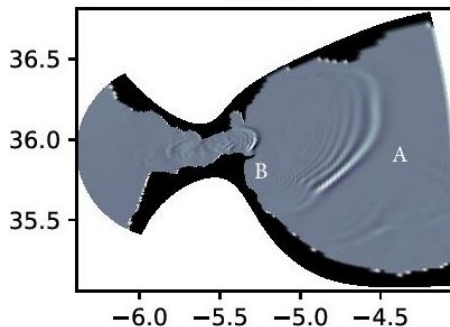
Known oceanographic features near Strait of Gibraltar



Terra, 22 May, 11:30 UTC
MODIS, Enhanced True Colour RGB.
Source: NASA EOSDIS Worldview



Western Alboran Gyre



Internal Waves

- Interested in recovering/decomposing known and hidden features
 - Gyres
 - Atlantic Jet
 - Internal waves
 - Hydraulic transitions
 - Special waves (such as Kelvin waves)
- Applied Dynamic Mode Decomposition (DMD) to simulated evolution

[Sánchez-Garrido, 2013], [Gofima UMA, YouTube],
[NASA EOSDIS Worldview]

Numerical Model

MIT general circulation model (MITgcm; [8]) (3-D, finite-volume) simulating the 3D velocity components, temperature, salinity and density.

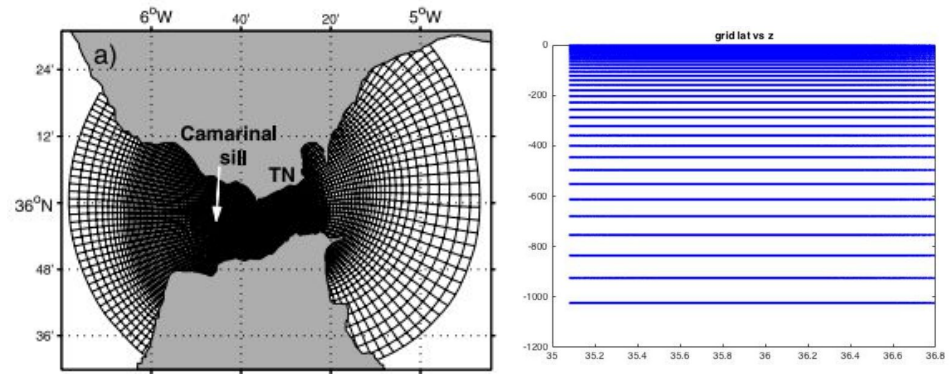
Input to analysis: velocity components at all grid points.

Grid:

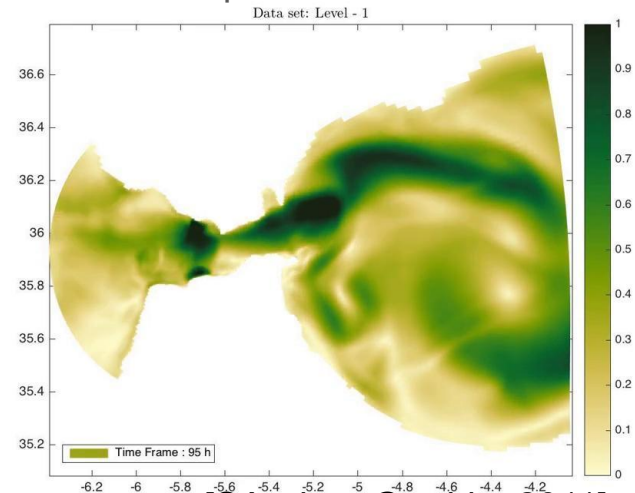
- Nonuniform curvilinear orthogonal grid (190 x 96 x 32 nodes)
- Duration of 144h (6 days) with time step 1h

Forcing: Tidal currents extracted from intermediate resolution model and prescribed at open boundaries:

- **diurnal** (O1, K1) tides,
- **semidiurnal** (M2, S2) barotropic tides.



Simulated surface speed:



[Sánchez-Garrido, 2011]

Dynamic Mode Decomposition (DMD)

Input Data

Let snapshot matrix $X = (S_i)$ where, S_i is column vector of state observable at step i

$$S_i := \begin{bmatrix} U_i \\ V_i \\ W_i \end{bmatrix}$$

$$X_1 = [S_1 \quad S_2 \dots S_{N-1}]$$

$$X_2 = [S_2 \dots S_{N-1} \quad S_N]$$

$$X_2 = \mathbb{K}X_1$$

where \mathbb{K} is koopman operator

$$\mathbb{K}_t[g](x) = g \circ f_t(x)$$

Why DMD?

- Isolate specific dynamic structures
- Equation free modeling
- Reduce the dimension of the data
- Simple algorithm and computation
- Can identify physically meaningful decomposition

Exact DMD

Input: X_1, X_2

- 1 $[U_r, \Sigma_r, V_r] = \text{SVD}(X_1)$; // Truncated SVD
- 2 $\mathbb{K} = U_r^* X_2 V_r \Sigma_r^{-1}$; // Compression $\mathbb{K} \downarrow \mathbb{K}$
- 3 $[\Psi, \Lambda] = \text{eig}(\mathbb{K})$; // $\text{diag}(\Lambda)$ equals to eigenvalues of \mathbb{K}
- 4 $\Phi = X_2 V_r \Sigma_r^{-1} \Psi$; // Φ estimates eigenvectors of \mathbb{K}
- 5 $\mathbf{b} = \Phi^\dagger X_1[:, 1]$; // Estimates the coefficients

Output: $\Phi, \Lambda, \mathbf{b}$

$$X(t) = \begin{bmatrix} u(t) \\ v(t) \\ w(t) \end{bmatrix} \approx \sum_{i=1}^r b_i \Phi_i(x, y, z) e^{\omega_i t} \quad \omega_i = \ln(\lambda_i) / \Delta t$$

Dynamic Mode Decomposition

Objective: Represent simulation data by a **linear, separation-of-variables data model**. Such linearization is **justified by Koopman operator theory**.

Spatiotemporal snapshot matrix

$$V(t, x) \approx \sum_{k=1}^K \Phi_k(x) \exp\{\Omega_k t\} b_k$$

Spatial profile
Time-evolution governed by eigenvalue
Mode magnitude

$$\Omega_k = \sigma_k + i\omega_k$$

DMD modes oscillate at a single (complex) time frequency.

Dominant modes: large mean L^2 norm

$$\tilde{b}_k := \frac{1}{T} \int_0^T |\exp\{\Omega_k t\} b_k|^2$$

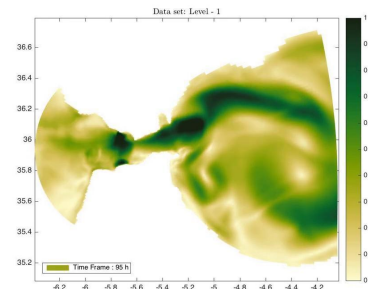
Real parts of eigenvalues imply growth/decay of a modes:

$$\text{sign Re } \Omega_k = \begin{cases} + & \text{Growth of mode} \\ - & \text{Decay of mode} \end{cases}$$

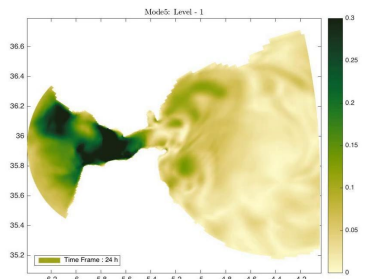
Imaginary parts of eigenvalues reported as oscillation period

$$P = 2\pi / \text{Im } \Omega_k$$

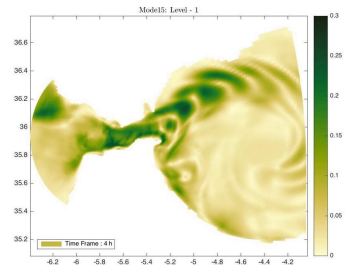
Input data:



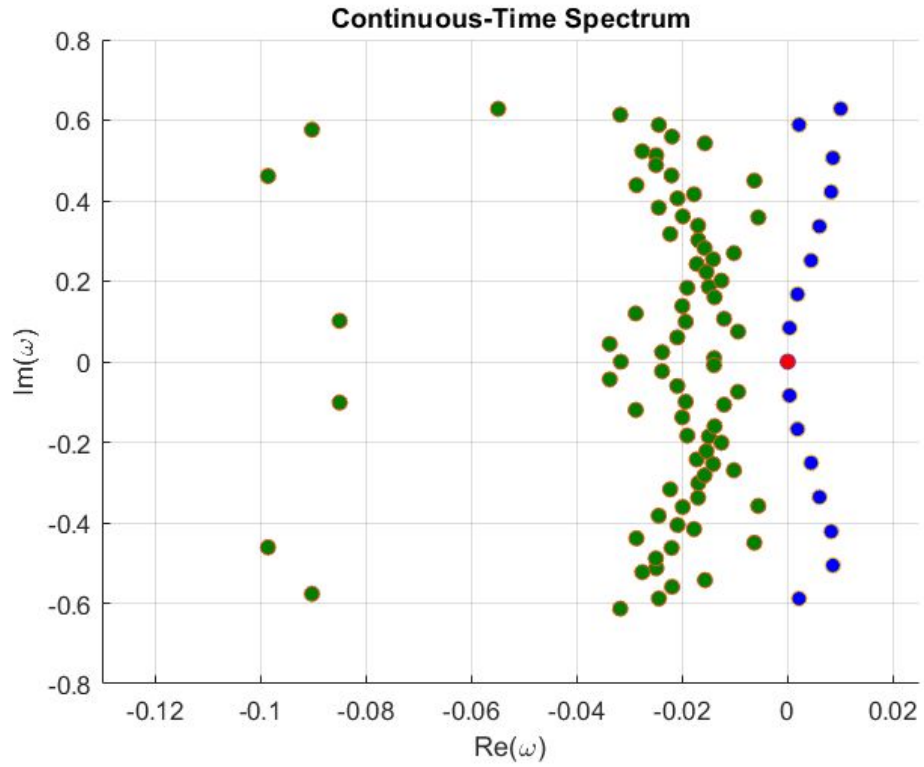
Semidiurnal dominant mode:



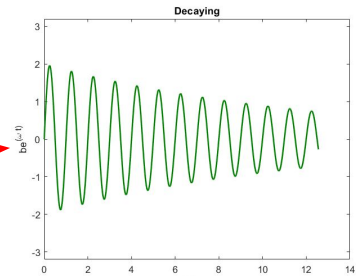
Diurnal dominant mode:



Behavior of Modes by Continuous-time Spectrum

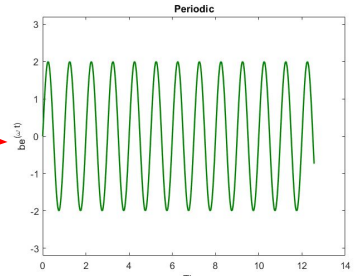


$Re(\omega) < 0$



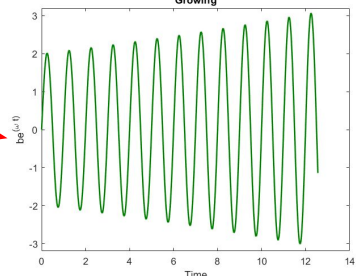
Decaying

$Re(\omega) = 0$



Periodic

$Re(\omega) > 0$

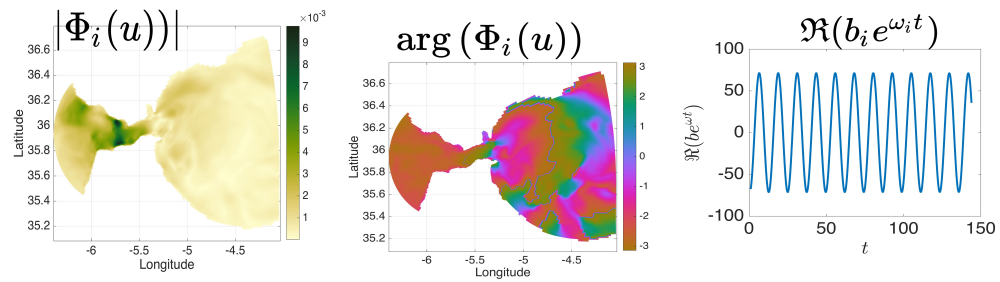


Growing

Best-Fit of Modes

$$X(t) = \begin{bmatrix} u(t) \\ v(t) \\ w(t) \end{bmatrix} \approx \sum_{i=1}^r b_i \Phi_i(x, y, z) e^{\omega_i t}$$

Let $\omega_i = \sigma_i + i\rho_i$



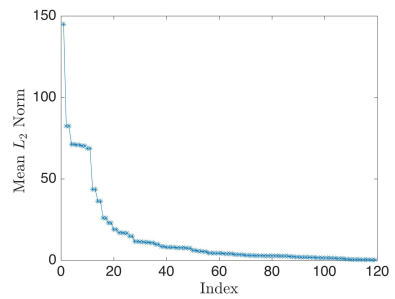
- DMD Algorithm decompose the data in to dynamical relevant flows features (same frequency).
- Noticed b, Φ, ω could be complex values.
- Eigenvalues ω describe the dynamics of the system.
- Magnitude and phase describes the how the spatial locations related each within a mode.

Mode Selection

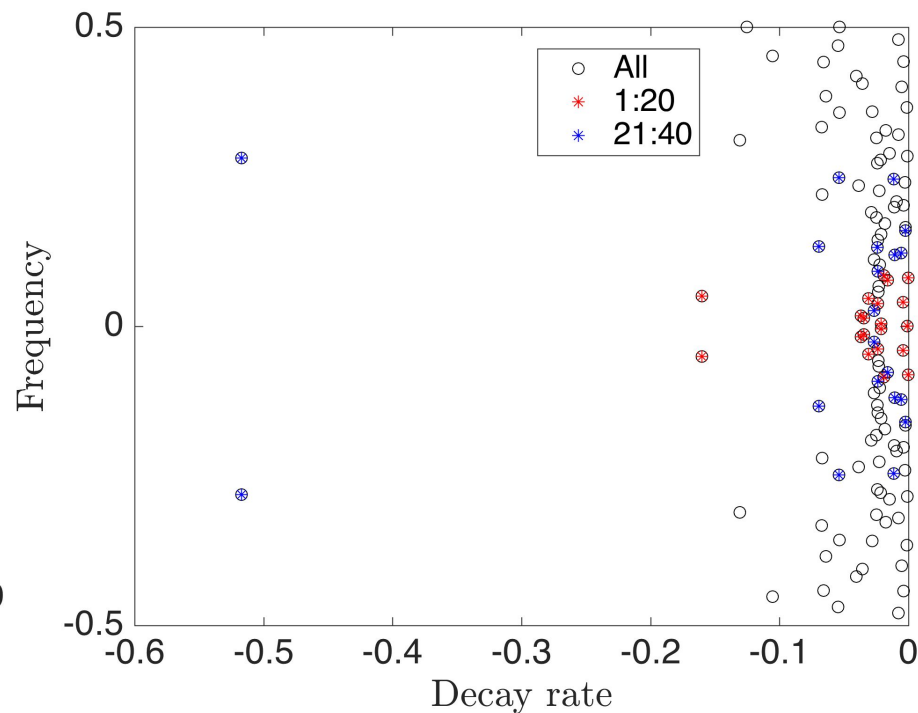
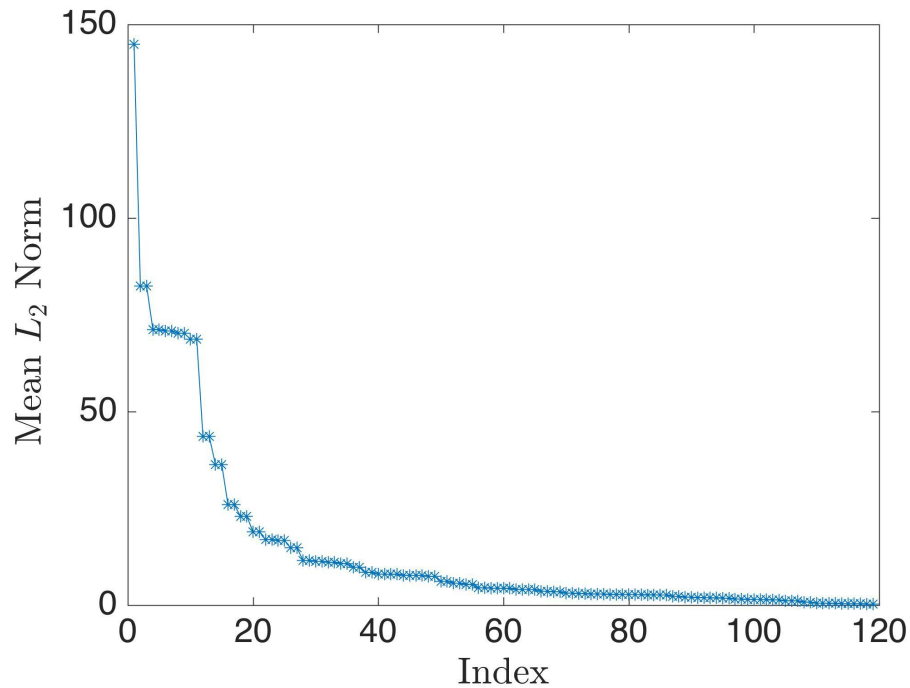
- L_2 norm contribution to the initial condition.
 - Sorting modes according to descending $|b|$.
- Average L_2 -contribution across all snapshots

$$E_i = \sqrt{\frac{1}{T} \int_0^T |b e^{\omega_i t}|^2 dt} = |b_i| \sqrt{\frac{e^{2\sigma_i T} - 1}{2\sigma_i T}}$$

- Selection of modes based on the oscillation frequency associated with eigenvalues enables matching of modes to frequencies known a priori, e.g., forcing frequencies.

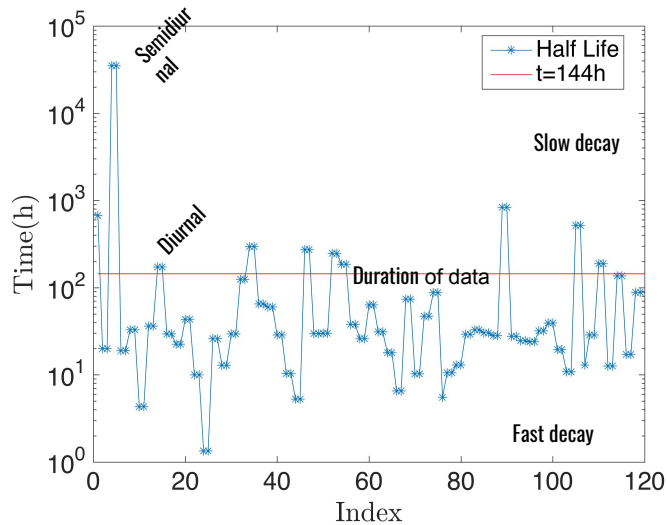


DMD for Gibraltar Dataset: Eigenvalue Spectrum



$$\omega_i = \ln(\lambda_i) / \Delta t$$

DMD Modes: Periods, decay rates, norms



Index	Half Life (h)	$P_i = \frac{2\pi}{\rho_i}$ (h)	Mean L2 Norm	b
1	668.10	Inf	144.84	155.63
3	19.91	73.47	82.44	259.25
5	35116.86	12.31	71.23	71.33
7	18.90	57.93	70.85	228.63
9	32.88	228.92	70.24	172.08
11	4.33	19.87	68.73	463.55
13	36.37	11.74	43.56	101.58
15	172.44	24.65	36.32	47.04
17	29.34	26.61	25.94	67.23
19	22.42	21.34	22.97	68.08
21	43.32	13.04	18.94	40.59
23	9.99	7.48	16.99	75.44
25	1.34	3.55	16.71	202.43
27	25.96	37.70	14.85	40.91
29	12.87	4.02	11.52	45.04
31	29.35	10.86	11.32	29.33
33	124.52	8.17	11.07	15.61
35	296.88	6.24	10.78	12.60
37	64.91	8.37	9.81	17.51
39	59.96	4.06	8.45	15.61
41	28.69	7.57	8.02	21.03
43	10.38	4.54	7.99	34.78
45	5.29	3.21	7.74	47.21
47	273.20	6.06	7.65	9.07
49	29.82	17.42	7.42	19.08

Tidal Component	Darwin	Period (hr)	Speed(°/hr)
Principal lunar semidiurnal	M_2	12.4206	28.9841
Principal solar semidiurnal	S_2	12	30
Smaller lunar elliptic diurnal	M_1	24.841	14.4921

Background mode

Semidiurnal

Diurnal

DMD mode 1 is approximately non-oscillatory.

DMD modes 5 related to M2 tidal mode.

Period of DMD mode 15 is equals to M1 tidal period.

Eigenvalue: $\omega_i = \sigma_i + i\rho_i$

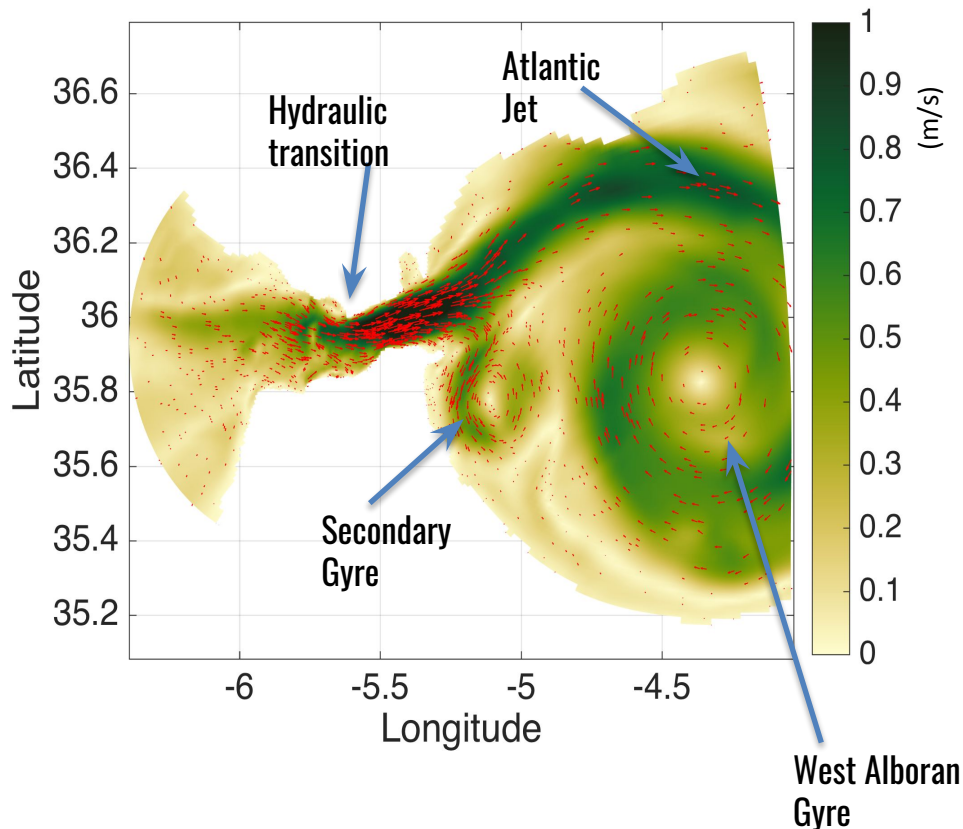
Half life Time(HLT): $\tau_i = \frac{-\ln(2)}{\sigma_i}$

Period: $P_i = \frac{2\pi}{\rho_i}$

Mean L_2 Norm: $\|E_i\| = \|\Phi_i\| \frac{2e^{2\sigma_i T} - 1}{2\sigma_i T}$

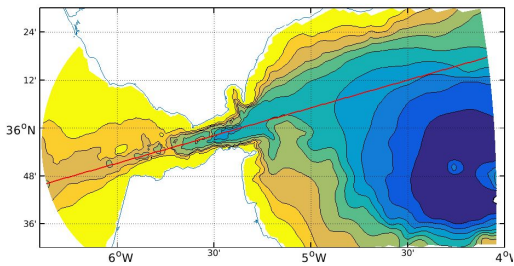
Mode 1: Non-oscillatory Background – Surface Speed

Fluid Speed, $\sqrt{u^2 + v^2}$ at the free surface.



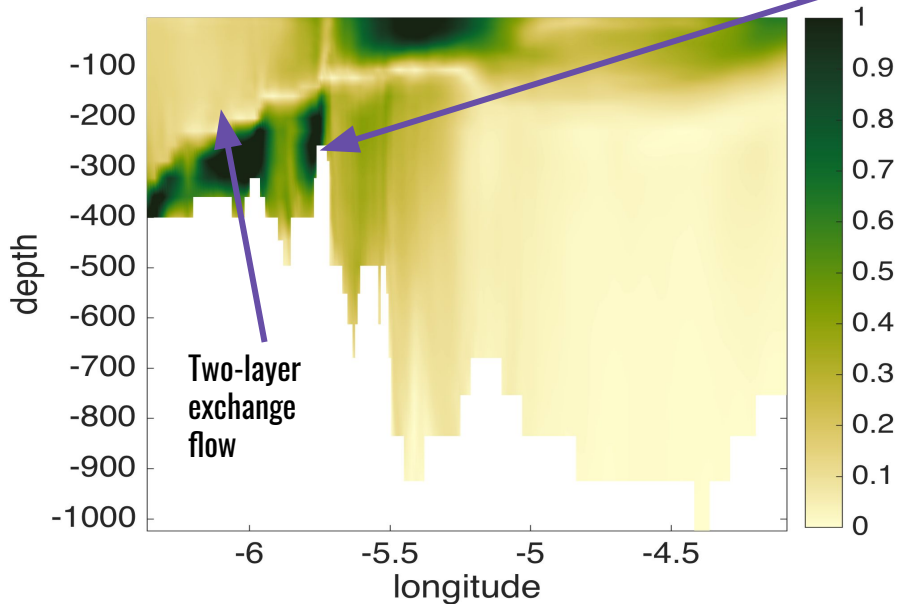
- Approximately non-oscillatory
- Persistent: Decay with half life time around 27 days (668 hours)
- Reveals several well-known features of the circulation in the region
 - West Alboran Gyre (WAG)
 - Atlantic Jet
 - the accelerated surface inflow in the Strait of Gibraltar.
- Also reveals a feature that is not as well known: secondary gyre that sits between the Ceuta and the WAG

Mode 1: Non-oscillatory Background – Vertical cross section

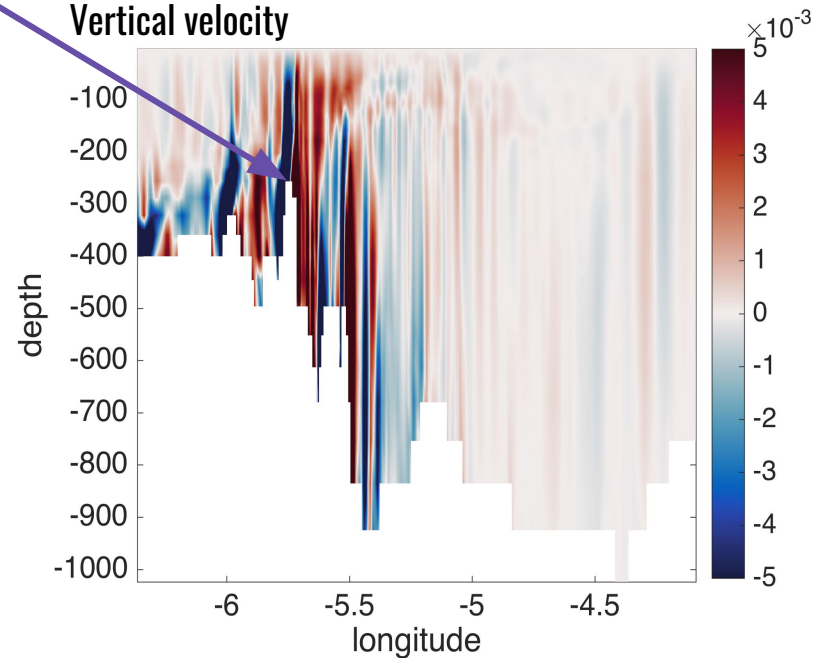


Hydraulic transition: westward flowing water spills over the Camarinal sill and gains speed

Horizontal speed

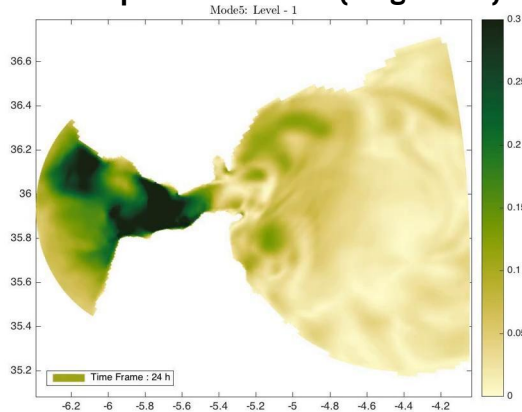


Vertical velocity

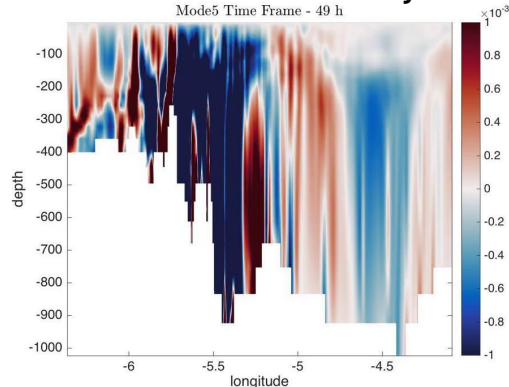


Mode 5: Dominant Semidiurnal (P=12.3 h)

Horiz. speed at surface (magnitude)

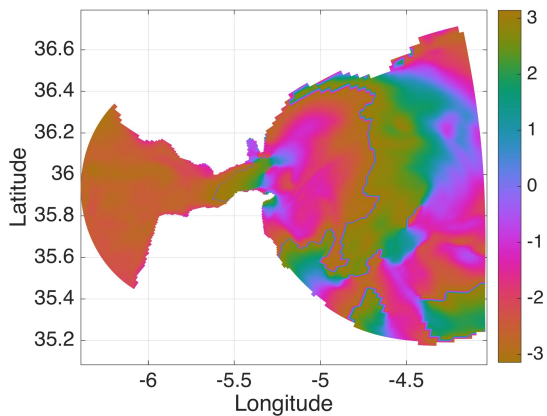


Cross-sec. vertical velocity

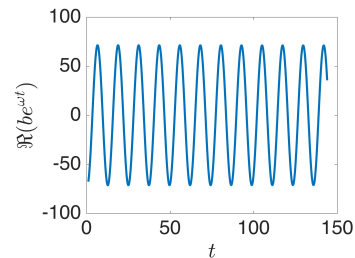
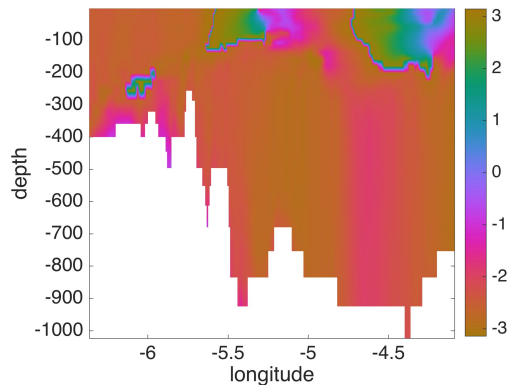


- Persistent: Effectively no decay
- Reveals internal waves radiating from the Strait into the Mediterranean.

Horiz. speed at surface (phase)

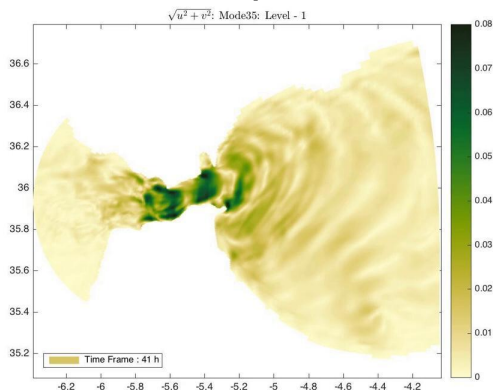


Cross-sec. vertical velocity phase

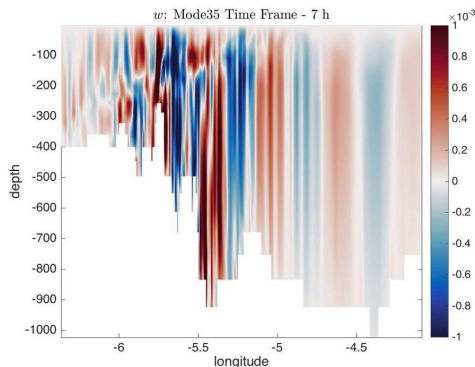


Mode 35: 2nd Harm. of Semidiurnal Tide (P=6.24h)

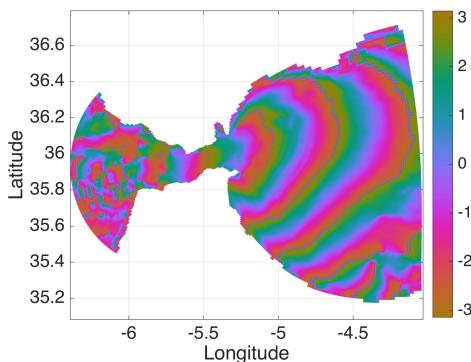
Surface horiz. speed magnitude



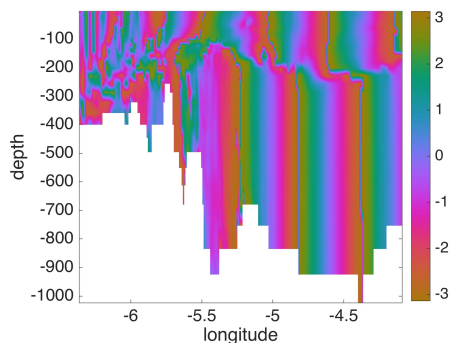
Cross-sec. vertical vel.



Surface horiz. speed phase



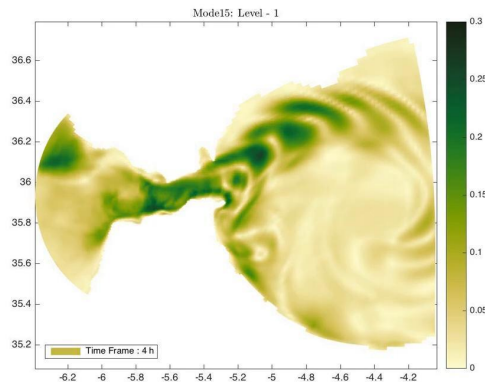
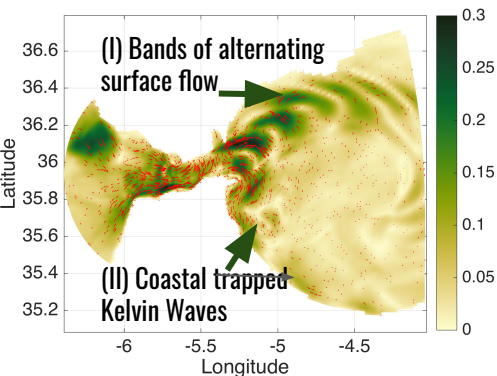
Cross-sec. vertical phase



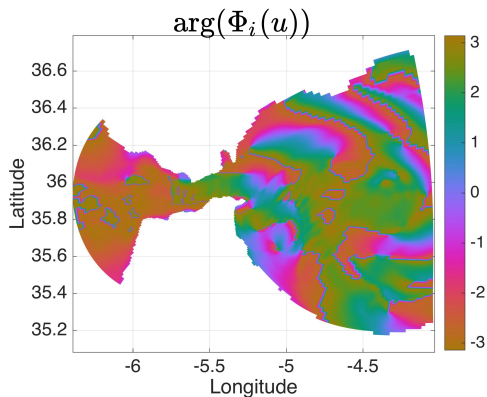
- Second harmonic of semidiurnal tide, and third harmonic of diurnal tides.
- Persistent: Decay with half life time around 297 hours (~2x available data length).
- Reveals internal waves radiating from the Strait into the Mediterranean.

Mode 15: Dominant Diurnal (P=24.65h) – Surface Section

Surface horiz. speed magnitude



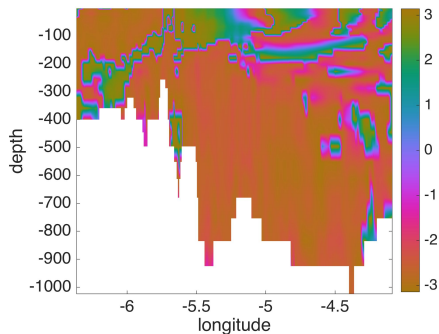
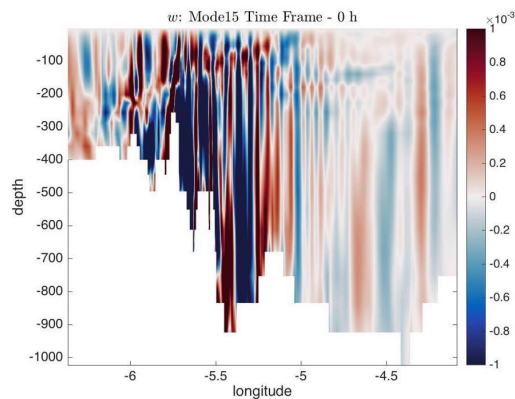
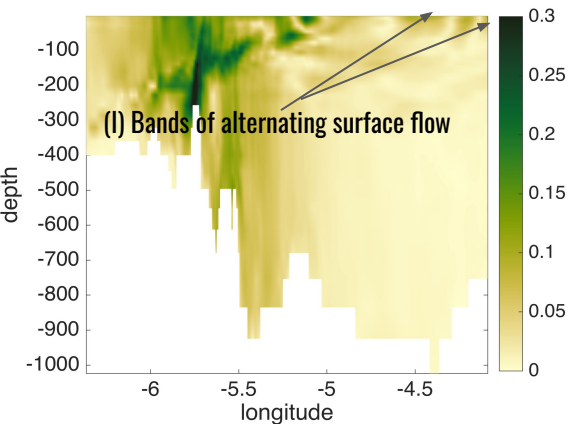
Surface horiz. speed phase



- Persistent: Decay half life around 172 h (7 days).
- (I) Isolates the meandering of the Atlantic Jet.
- Indicates that Atlantic Jet meanders are locked with a tide (first observation?).
- (II) Shows two patches of strong horizontal surface velocity along the southern coastline (Kelvin waves)

Hypothesis: Meanders originate from tidal pulses of vorticity generated in the strait and then carried by the jet.

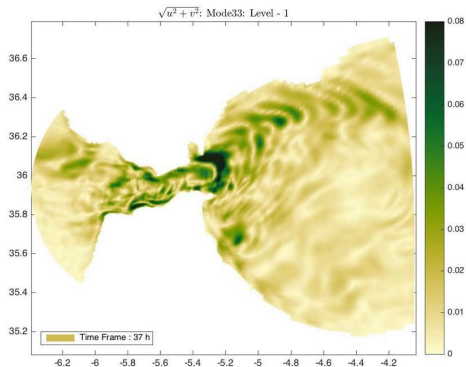
Mode 15: Dominant Diurnal (P=24.65h) – Vertical Section



- Persistent: Decay half life around 172 h (7 days).
- (I) Isolates the meandering of the Atlantic Jet.
- Indicates that Atlantic Jet meanders are locked with a tide (first observation?).
- (II) Shows two patches of strong horizontal surface velocity along the southern coastline (Kelvin waves)

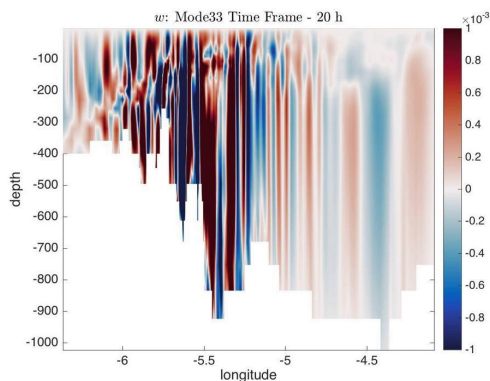
Mode 33: 3rd Harm. of Diurnal Tide (P=8.17h)

Horiz. speed at surface (magnitude)



←
**Meandering
of the
Atlantic Jet**

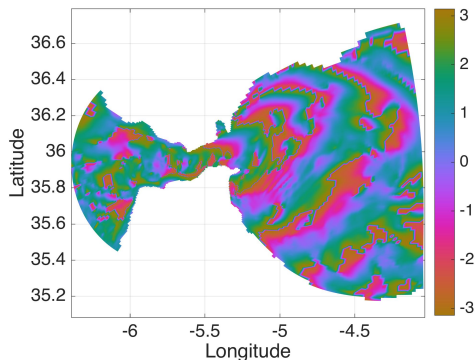
Cross-sec. vertical velocity



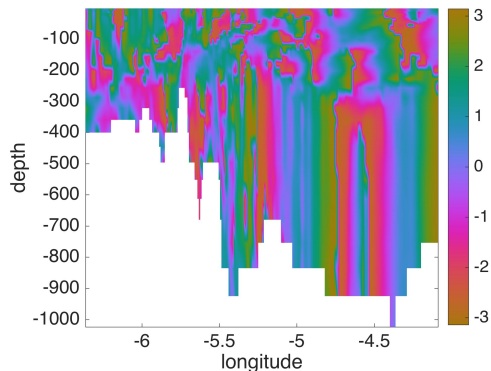
- Persistent: Decay with half life time around 124 hours.
- Exhibits internal wave activity and shows additional detail in Atlantic Jet meandering.

Horiz. speed at surface (phase)

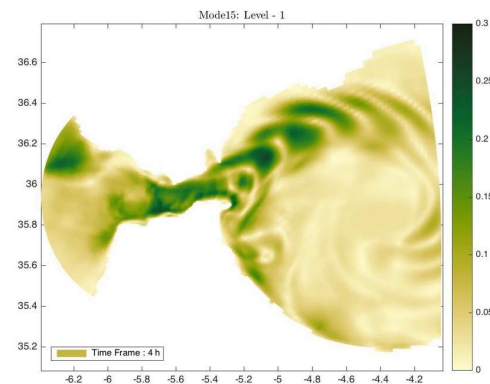
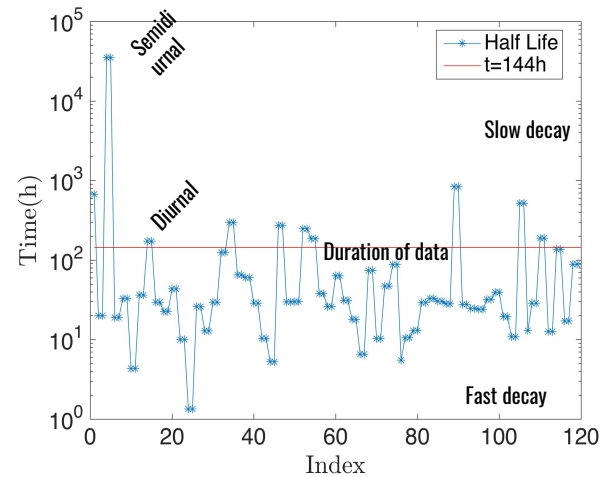
$$\arg(\Phi; (u))$$



Cross-sec. vertical velocity phase



- Dynamic Mode Decomposition decomposes the data into modes that evolve according to a single (complex-valued) frequency.
- Clear time signature enables easy correlation with tidal components and identification of tidal harmonics.
- Individual DMD modes correlate with specific features and mechanisms of ocean dynamics: West Alboran Gyre, Atlantic Jet, hydraulic transition at Camarinal Sill, radiating internal waves, ...
- DMD modes additionally isolate less-obvious features: secondary gyre at Ceuta, hydraulic jump, meandering of Atlantic Jet, Kelvin waves.



- [1] Erik M. Bollt, “Geometric Considerations of a Good Dictionary for Koopman Analysis of Dynamical Systems”, preprint arXiv:1912.09570 (2020)
- [2] J. C. Sánchez-Garrido, J. G. Lafuente, E. Álvarez Fanjul, M. G. Sotillo, and F. J. de los Santos, “What does cause the collapse of the western alboran gyre? results of an operational ocean model”, *Progress in Oceanography* 116, 142–153 (2013)
- [3] J. G. Lafuente, J. Almazán, F. Castillejo, A. Khribeche, and A. Hakimi, “Sea level in the strait of gibraltar: tides”, *The International Hydrographic Review* 67(1990).
- [4] M. Budišić, R. Mohr, and I. Mezić, “Applied Koopmanism”, *Chaos. An Interdisciplinary Journal of Nonlinear Science* 22, 047510, 33 (2012).
- [5] Taira, K., Brunton, S. L., Dawson, S., Rowley, C. W., Colonius, T. and McKeon, B. J., Schmidt, O. T., Gordeyev, S., Theofilis, V. & Ukeiley, L. S. 2017 Modal analysis of fluid flows: An overview. *AIAA J.* 55 (12), 4013–4041.
- [6] C. W. Rowley, I. Mezić, S. Bagheri, P. Schlatter, and D. S. Henningson, “Spectral analysis of nonlinear flows”, *Journal of Fluid Mechanics* 641, 115–127 (2009)
- [7] J. N. Kutz, S. L. Brunton, D. M. Luchtenburg, C. W. Rowley, and J. H. Tu, “On dynamic mode decomposition: theory and applications”, *Journal of Computational Dynamics* 1, 391–421 (2014).
- [8] John Marshall, Alistair Adcroft, Chris Hill, Lev Perelman, and Curt Heisey, A finite-volume, incompressible navier-stokes model for studies of the ocean on parallel computers, *Journal of Geophysical Research: Oceans* 102(1997)
- [9] Sánchez-Garrido, J. C; Sannino, G; Liberti, L; García Lafuente, J; Pratt, L. *Journal of Geophysical Research. Oceans*; Washington Vol. 116, Iss. 12, (2011).
- [10] Jonathan H. Tu, Clarence W. Rowley, Dirk M. Luchtenburg, Steven L. Brunton, and J. Nathan Kutz, On dynamic mode decomposition: Theory and applications, *Journal of Computational Dynamics* 1 (2014), no. 2, 391–421. MR3415261